Available online at www.sciencedirect.com
ScienceDirect
Journal of Solid State Chemistry 179 (2006) 3575–3581
JOURNAL OF SOLID STATE CHEMISTRY
www.elsevier.com/locate/jssc

Magnetic properties of lanthanide rhenium oxides Ln_3ReO_7 (Ln = Sm, Eu, Ho)

Makoto Wakeshima, Yukio Hinatsu*

Division of Chemistry, Graduate School of Science, Hokkaido University, Sapporo 060-0810, Japan

Received 8 June 2006; received in revised form 21 July 2006; accepted 22 July 2006
Available online 27 July 2006

Abstract

Ternary lanthanide rhenium oxides Ln_3ReO_7 (Ln = Sm, Eu, Ho) were prepared and their structures were determined by X-ray diffraction measurements. They crystallize in an orthorhombic superstructure of cubic fluorite (space group *Cmcm* for Ln = Sm, Eu; $C222_1$ for Ln = Ho). The magnetic properties were characterized by magnetic susceptibility and specific heat measurements from 1.8 to 400 K. The Sm_3ReO_7 shows an antiferromagnetic transition at 1.9 K. The Eu_3ReO_7 indicates a magnetic anomaly at 12 K. On the other hand, the results of the specific heat measurements indicate that both Sm_3ReO_7 and Eu_3ReO_7 undergo a structure transition at 270 and 350 K, respectively. The Ho_3ReO_7 is paramagnetic down to 1.8 K.

Keywords: Magnetic properties; Lanthanide; Rhenium; Oxides; Magnetic susceptibility; Specific heat; Structure transition

1. Introduction

In recent years, the solid-state chemistry of mixed-metal oxides containing both lanthanides (4*f* metals) and 4*d* or 5*d* transition metals has attracted a great deal of interest. These materials adopt a diverse range of structures and show a wide range of electronic properties due to 4*f* and 4*d* (or 5*d*) electrons. We have focused our attention on the structural chemistry and magnetic properties of compounds with general formula Ln_3MO_7 (Ln = lanthanides, M = 4*d* or 5*d* transition metals). The parent structure of this family of compounds, La_3NbO_7, was first determined by Rossell [1]. The structure is an orthorhombic superstructure of the cubic fluorite-type (lattice parameter a_c) with space group *Cmcm* and unit-cell parameters $a_{orth} \approx 2a_c$, $b_{orth} \approx c_{orth} \approx \sqrt{2}a_c$. There are three distinct cation sites, one distorted cubic Ln^{3+} site, one distorted pentagonal bipyramidal Ln^{3+} site and one octahedral M^{5+} site. The M^{5+} cation is octahedrally coordinated by six oxygen ions and the octahedra share corners forming a zig-zag chain parallel to the *c*-axis. In this structure, slabs are formed in the *bc* plane, in which one-dimensional MO_6 chain runs parallel to the *c*-axis alternating with rows of edge-shared LnO_8 pseudo-cubes consisting of one third of Ln ions. These slabs are separated by the remaining two thirds of Ln ions which is seven-coordinated by oxygen ions. The interchain M–M distance is about 6.6 Å compared with the corresponding intrachain distance of 3.7 Å, which suggests that these compounds may exhibit one-dimensional electronic behavior. In addition, since most of the lanthanides have a nonzero spin, this could lead to long-range order due to Ln–M coupling at some finite temperatures.

Due to this unique crystal structure and possible related magnetic properties, many studies have been performed, especially for the magnetic properties of compounds containing Ru at the M site [2–10]. Recently, detailed magnetic and thermal investigations were reported for the ruthenium-, iridium- and osmium-containing members of the Ln_3MO_7 family and provided evidence for the existence of low-temperature structural phase transitions [8–13].

As for Ln_3ReO_7 compounds, Wltschek et al. [14] first analyzed the crystal structure of Sm_3ReO_7 by measuring the X-ray diffraction with a single crystal, and the crystal structure was found to be orthorhombic with space group

*Corresponding author. Fax: +81 11 706 2702.
E-mail address: hinatsu@sci.hokudai.ac.jp (Y. Hinatsu).

0022-4596/$ - see front matter © 2006 Elsevier Inc. All rights reserved.
doi:10.1016/j.jssc.2006.07.033

Cmcm. Magnetic susceptibility measurements showed that Sm_3ReO_7 was paramagnetic down to 4 K. For Pr_3ReO_7 and Nd_3ReO_7, Lam et al. [15] also refined the structures with the same space group *Cmcm*. In these two compounds, the Re^{5+} ions display a local magnetic moment consistent with $S = 1$ and both show evidence for cooperative magnetic effects at low temperatures. We reported the structure and magnetic properties of Ln_3ReO_7 (Ln = Gd, Tb and Dy) [16]. They crystallize in an orthorhombic superstructure of cubic fluorite (space group *Cmcm* for Ln = Gd, Tb; $C222_1$ for Ln = Dy). These Ln_3ReO_7 (Ln = Gd, Tb and Dy) compounds show magnetic transitions at 8.0, 17 and 2.8 K, respectively. Below the transition temperatures, there is a large difference in the temperature dependence of the magnetic susceptibility measured between under zero-field-cooled condition and under field-cooled condition. This series of compounds Ln_3ReO_7 is also expected to show low-temperature structural phase transitions because the ionic radius of Re^{5+} is close to that of Os^{5+} [17].

In this study, we extended the preparation of Ln_3ReO_7 to Ln = Sm, Eu and Ho. Through X-ray diffraction measurements, their crystal structures were determined. The magnetic susceptibility and specific heat measurements were performed from 1.8 to 400 K in order to elucidate their magnetic properties and to check the existence of the structure transition in the Ln_3ReO_7 series.

2. Experimental

2.1. Sample preparation

As starting materials, Ln_2O_3, ReO_2 and ReO_3 were used. They were weighed in an appropriate metal ratio and were ground in an agate mortar. The mixtures were pelletized and sealed in an evacuated platinum tube, and then heated at 1000–1200 °C for 6–12 h. With several intermediate regrindings and repelletizing, the products were annealed at the same temperature until a single Ln_3ReO_7 phase was obtained. For the preparation of Ho_3ReO_7, it was needed to heat the specimen at 1350–1400 °C.

2.2. X-ray diffraction analysis

Powder X-ray diffraction measurements were performed in the region of $10° \leqslant 2\theta \leqslant 120°$ using Cu$K\alpha$ radiation on a Rigaku MultiFlex diffractometer equipped with a curved graphite monochromator. The Rietveld analyses were carried out with the program RIETAN-2000 [18] using collected diffraction data.

2.3. Magnetic susceptibility measurements

The temperature dependence of the magnetic susceptibility was measured in an applied field of 0.1 T over the temperature range of $1.8\,K \leqslant T \leqslant 400\,K$, using a SQUID magnetometer (Quantum Design, MPMS5S). The susceptibility measurements were performed under both zero-field-cooling (ZFC) and field-cooling (FC) conditions. The former was measured upon heating the sample to 400 K under the applied magnetic field of 0.1 T after ZFC to 1.8 K. The latter was measured upon cooling the sample from 400 to 1.8 K at 0.1 T.

2.4. Specific heat measurements

Specific heat measurements were performed using a relaxation technique by a commercial heat capacity measuring system (Quantum Design, PPMS) in the temperature range of 1.8–400 K. The sintered sample in the form of a pellet was mounted on a thin alumina plate with Apiezon for better thermal contact.

3. Results and discussion

3.1. Preparation and crystal structure

X-ray diffraction measurements show that desired compounds Ln_3ReO_7 (Ln = Sm, Eu and Ho) could be prepared and that very small amounts of impurities remained in the desired compounds; they were unreacted starting materials Ln_2O_3. This is presumably a consequence of the loss of more volatile rhenium oxides. In order to remove these impurities, the samples were washed with diluted hydrochloric acid. After this treatment, the single-phase compounds could be obtained.

Figs. 1(a) and (b) show the X-ray diffraction profiles for Eu_3ReO_7 and Ho_3ReO_7, respectively. They indicate that these two compounds have mutually distinct crystal structures. Wltschek et al. [14] analyzed the crystal structure of Sm_3ReO_7 by measuring the X-ray diffraction with a single crystal, and the crystal structure is found to be orthorhombic with space group *Cmcm*. Later, Lam et al. [15] refined the structures of Pr_3ReO_7 and Nd_3ReO_7 with the same space group *Cmcm*. We also analyzed the structures of Gd_3ReO_7 and Tb_3ReO_7 with the same space group [16]. The crystal structure of Eu_3ReO_7 was well refined with the space group *Cmcm*. Table 1 lists the lattice parameters and atomic coordinates for Eu_3ReO_7. For the X-ray diffraction profile of Ho_3ReO_7, there exist many very weak $h\,0\,l$ reflections with odd l, which could not be indexed based on the *Cmcm* or other space groups such as *Pnma* (for La_3NbO_7) [19] and $P2_12_12_1$ (for Ln_3MoO_7) [20]. Allpress and Rossell [21] reported that the crystal structures of Ln_3MO_7 (M = Ta, Sb) for smaller Ln cations were well described with space group $C222_1$, and Rossell [1] analyzed the detailed crystal structure of Y_3TaO_7. We also analyzed the X-ray diffraction profile for Dy_3ReO_7 with space group $C222_1$ [16]. All the reflections observed for Ho_3ReO_7 could be successfully indexed with the same space group $C222_1$. The refinement by using the Y_3TaO_7-type structural model converged rapidly, and yielded low residual factors and acceptably low values for the calculated standard deviations of refined parameters.

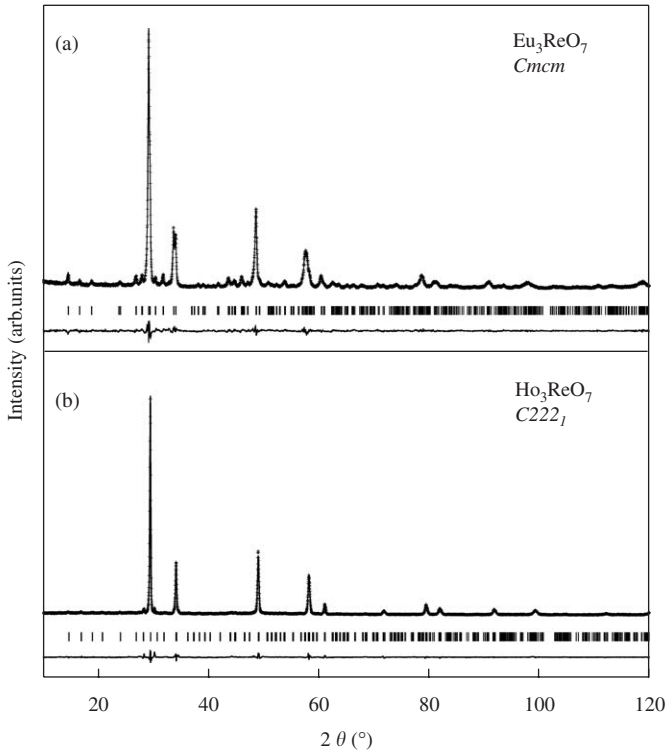

Fig. 1. Powder X-ray diffraction profiles for (a) Eu_3ReO_7 and (b) Ho_3ReO_7. The calculated and observed profiles are shown on the top solid line and cross markers, respectively. The vertical marks in the middle show positions calculated for Bragg reflections. The lower trace is a plot of the difference between calculated and observed intensities.

Table 1 also lists the lattice parameters and atomic coordinates for Ho_3ReO_7.

Fig. 2 illustrates the crystal structures of Eu_3ReO_7 and Ho_3ReO_7. The orthorhombic structures have features in common for both the compounds. The ReO_6 octahedra share the O(3) (for Eu_3ReO_7) and O(5) (for Ho_3ReO_7) ions and form an infinite one-dimensional zig-zag chain parallel to the [001] direction. The *Ln*(1) ions are coordinated by eight oxygen ions and the distorted *Ln*(1)O_8 cubes also form an one-dimensional chain through edge sharing. The ReO_6 and *Ln*(1)O_8 chains lie alternately parallel to the (010) plane and the *Ln*(2) ions are seven-coordinated by oxygen ions between the slabs consisting of these chains. The ReO_6 octahedron and *Ln*(1)O_8 cube in the Eu_3ReO_7 structure are more regular than those in the Ho_3ReO_7 structure. The ReO_6 octahedra in the Eu_3ReO_7 and Ho_3ReO_7 structures are tilted along the [010] and [100] directions, respectively.

Fig. 3 shows the specific heat for Sm_3ReO_7 and Eu_3ReO_7 in the wide temperature range of 1.8–400 K. The specific heat data show a broad peak at 270 K for Sm_3ReO_7 and at 345 K for Eu_3ReO_7. We consider that these thermal anomalies are due to a structure transition. We reported the existence of low-temperature structure transitions for the Ln_3MO_7 (*Ln* = Ru, Ir, Mo) series [8–11,22], and pointed out that these structure transition temperatures increase with decreasing the ionic radius of *Ln*. Gemmill et al. [12,13] also observed the structure transitions for *Ln* = Ru, Os compounds with space group *Cmcm* and

Table 1
Crystal structure data for Eu_3ReO_7 and Ho_3ReO_7

	Site	*x*	*y*	*z*	*B* (Å^2)
Eu_3ReO_7					
Space group: *Cmcm*		$a = 10.634(1)$ Å, $b = 7.3955(7)$ Å, $c = 7.4786(8)$ Å			
$R_I = 2.24\%$, $R_{wp} = 9.84\%$					
Eu(1)	4*a*	0	0	0	1.5(2)
Eu(2)	8*g*	0.2288(2)	0.2943(2)	1/4	0.4(2)
Re	4*b*	0	1/2	0	0.1(5)
O(1)	4*c*	0	0.441(3)	1/4	1.5(2)
O(2)	16*h*	0.1363(9)	0.295(1)	0.035(1)	1.5
O(3)	8*g*	0.132(1)	0.022(2)	1/4	1.5
Ho_3ReO_7					
Space group: $C222_1$		$a = 10.483(1)$ Å, $b = 7.4339(6)$ Å, $c = 7.4432(7)$ Å			
$R_I = 4.39\%$, $R_{wp} = 8.38\%$					
Ho(1)	4*b*	0	0.4956(2)	1/4	0.97(7)
Ho(2)	8*c*	0.2356(2)	0.2372(2)	0	0.80(6)
Re	4*b*	0	0	1/4	0.40(6)
O(1)	8*c*	0.139(1)	0.181(1)	0.304(1)	0.73(10)
O(2)	8*c*	0.121(1)	0.770(1)	0.2367(1)	0.73
O(3)	4*a*	0.131(1)	1/2	0	0.73
O(4)	4*a*	0.131(1)	1/2	1/2	0.73
O(5)	4*a*	0.072(1)	0	0	0.73

Note: $R_{wp} = \left[\sum_i w_i\left(y_i - f_i(x)\right)^2 / \sum_i w_i y_i^2\right]^{1/2}$ and

$R_I = \sum |I_k(o) - I_k(c)| / \sum I_k(o)$.

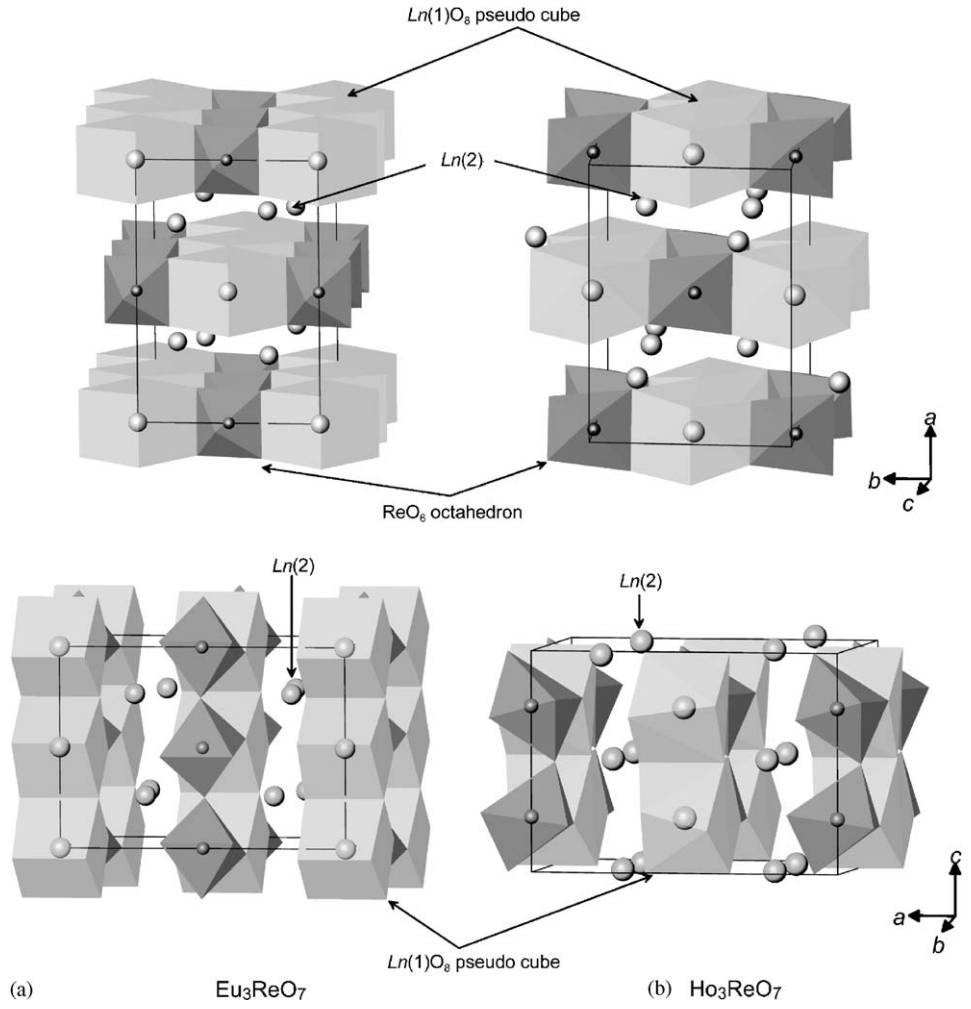

Fig. 2. Crystal structures of Ln_3ReO_7: (a) Eu_3ReO_7; (b) Ho_3ReO_7.

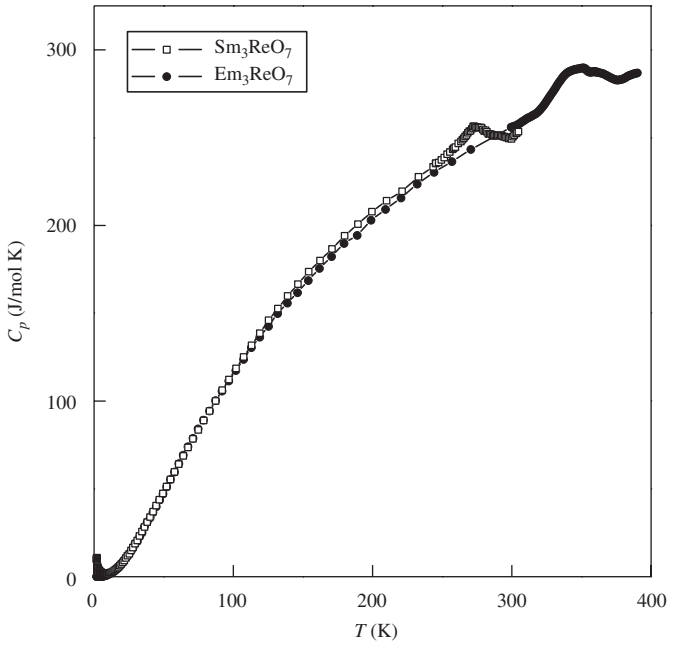

Fig. 3. Specific heat for Sm_3ReO_7 and Eu_3ReO_7 in the temperature range of 1.8–400 K.

determined the low-temperature crystal structure. Since the ionic radius of Re^{5+} is close to that of Os^{5+} [17], the structure transition temperatures for Ln_3ReO_7 and Ln_3OsO_7 should be comparable between them. Fig. 4 shows the variation of the structure transition temperatures for Ln_3MO_7 against the ionic radius of Ln^{3+}, which supports our expectation. For each of the five series of Ln_3MO_7 compounds, the structure transition temperatures decrease with increasing the ionic radius of Ln^{3+}. Each transition temperature within a series is separated by approximately the same temperature interval except for the case of Ln_3MoO_7 (Ln = Sm, Eu).

3.2. Magnetic properties

3.2.1. Sm_3ReO_7

Wltschek et al. [14] measured the magnetic susceptibility of Sm_3ReO_7 down to 4.2 K and reported that this compound was paramagnetic and its magnetic susceptibility was described by a Curie–Weiss law modified by a temperature-independent van Vleck paramagnetism. We performed the susceptibility measurements down to 1.8 K. Fig. 5(a) shows the low-temperature dependence of the

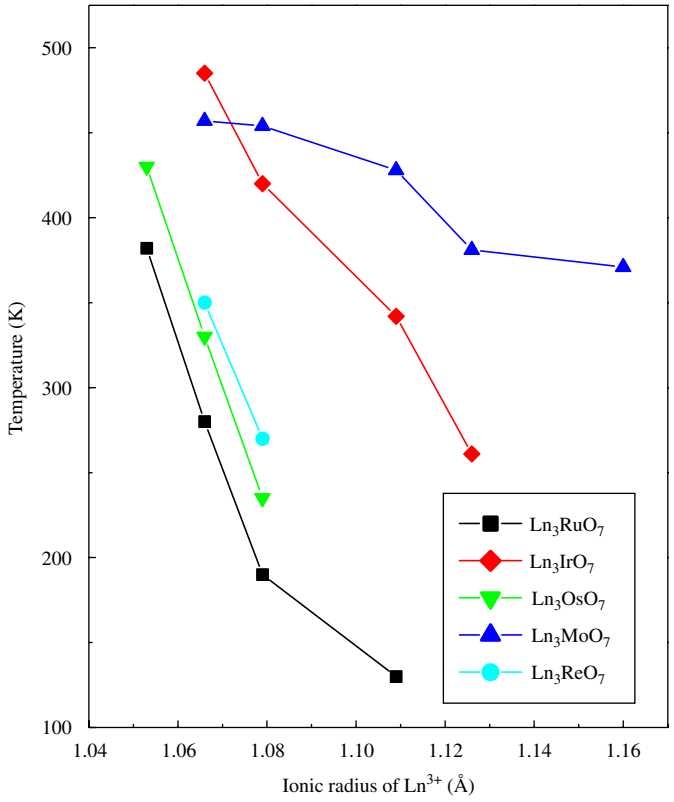

Fig. 4. Structure transition temperature vs. ionic radius of Ln^{3+} in eight coordination for Ln_3MO_7 (M = Mo, Ru, Re, Os, Ir).

magnetic susceptibilities for Sm_3ReO_7 below 20 K. A divergence between the ZFC and FC magnetic susceptibilities is found below 12 K, and a bend in the χ vs. T curve is observed at 1.9 K (see the arrow in the figure). At higher temperatures, Sm_3ReO_7 exhibits almost the temperature-independent van Vleck paramagnetism, as shown in the inset of Fig. 5(a).

Fig. 5(b) shows the low-temperature dependence of the specific heat divided by temperature (C_p/T). A clear peak is observed at 1.9 K, indicating a long-range magnetic ordering, and this anomaly is consistent with the bend at 1.9 K observed in the χ vs. T curve. The $^6H_{5/2}$ ground state of Sm^{3+} is expected to split into three Kramers doublets in the orthorhombic symmetry [23]. The magnetic anomaly at 1.9 K is due to an antiferromagnetic ordering which is caused by the low-lying Kramers doublet.

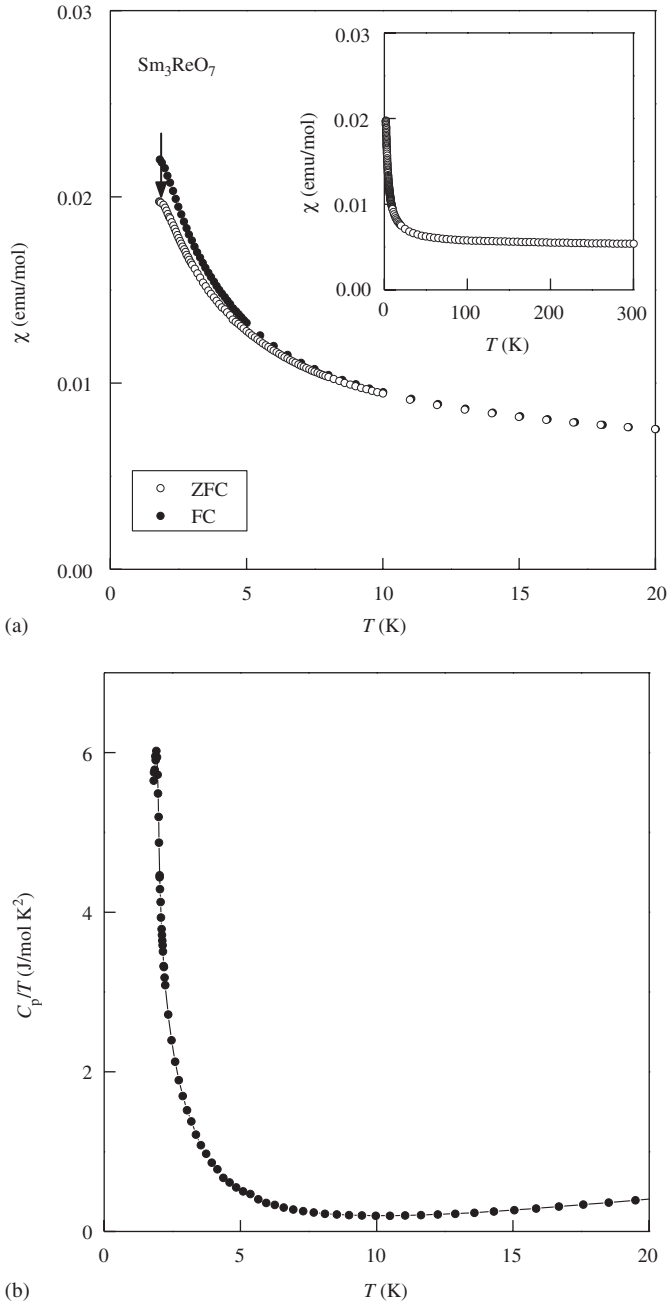

Fig. 5. (a) Magnetic susceptibility vs. temperature curve for Sm_3ReO_7 below 20 K. The inset shows the temperature dependence of magnetic susceptibility in the temperature range from 1.8 to 300 K. (b) Temperature dependence of specific heat divided by temperature (C_p/T) for Sm_3ReO_7 below 20 K.

3.2.2. Eu_3ReO_7

Fig. 6(a) shows the temperature dependence of the magnetic susceptibility for Eu_3ReO_7. The susceptibility increases with decreasing temperature and its increase becomes rapid when the temperature is decreased through ca. 20 K. A small divergence between the ZFC and FC magnetic susceptibilities is observed below ca. 12 K (see the inset of Fig. 6(a)). Since the ground state of Eu^{3+} ion is $^7F_0$, i.e., nonmagnetic, the Eu^{3+} ion does not contribute to the temperature dependence of magnetic susceptibility at low temperatures. In fact, the magnetic susceptibility for Eu_3TaO_7 (Ta^{5+}: diamagnetic) attains a constant value below 50 K [24]. Therefore, the rapid increase of magnetic susceptibility and the anomaly below 12 K for Eu_3ReO_7 should be due to the magnetic contribution from the Re^{5+} ions.

Fig. 6(b) shows the temperature dependence of the specific heat divided by temperature (C_p/T) below 30 K for Eu_3ReO_7. The C_p/T data for Eu_3TaO_7 are also plotted in the same figure, for comparison. The energy difference between the ground $^7F_0$ state and the first excited state $^7F_1$

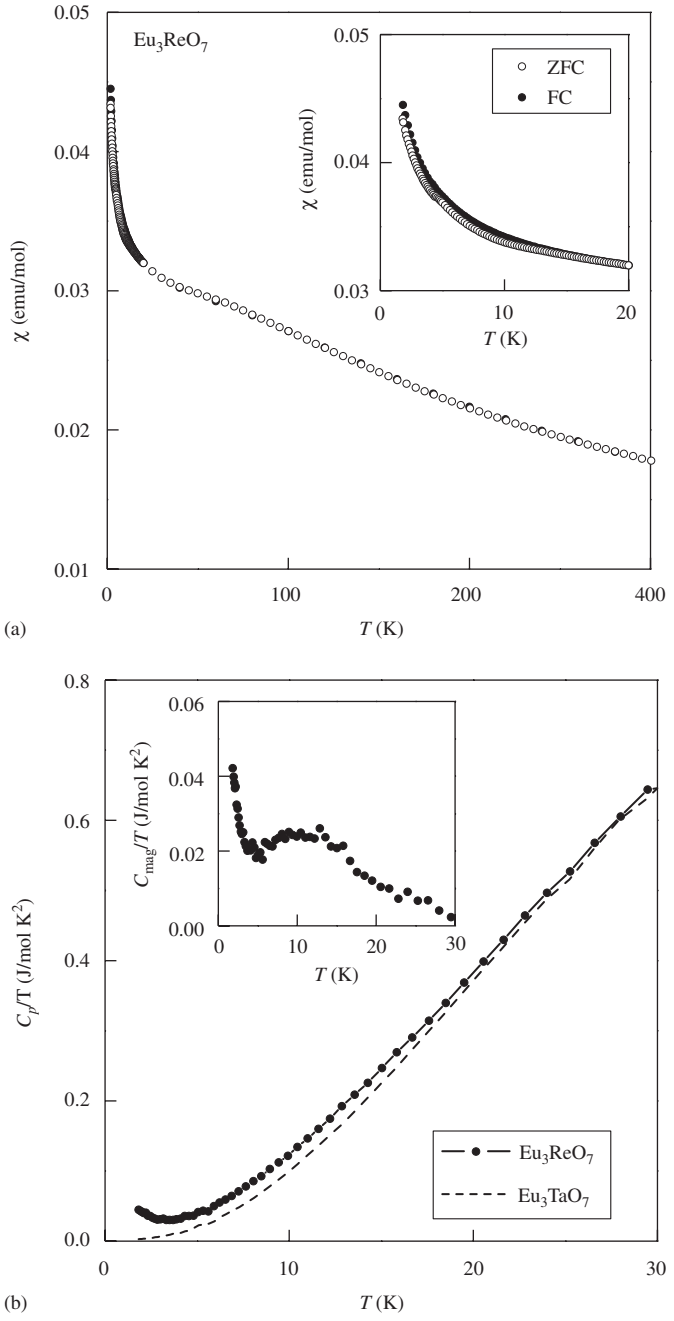

Fig. 6. (a) Temperature dependence of magnetic susceptibility for Eu_3ReO_7. The inset shows its detailed temperature dependence below 20 K. (b) Temperature dependence of specific heat divided by temperature (C_p/T) for Eu_3ReO_7 below 30 K. A broken line shows the C_p/T for Eu_3TaO_7, for comparison. The inset shows the temperature dependence of magnetic specific heat divided by temperature (C_{mag}/T) below 30 K.

for the Eu^{3+} ion is about 300 K [25]. For the insulating Eu_3TaO_7, the contribution from the Schottky-type and electronic specific heats to the total specific heat should be negligible, i.e., the specific heat for Eu_3TaO_7 is due to the lattice contribution. Actually, the C_p/T of Eu_3TaO_7 converges to 0 J/K^2/mol when the temperature is decreased to 0 K, as shown in Fig. 6(b). On the other hand, the experimental results for Eu_3ReO_7 show that the total specific heat clearly increases with decreasing temperature below 3 K. We consider that this is ascribable to the magnetic interactions of Re^{5+} ions. To estimate the magnetic contribution of the Re^{5+} ions to the total specific heat of Eu_3ReO_7, C_{mag}, we subtracted the specific heat of Eu_3TaO_7 from that of Eu_3ReO_7. The inset of Fig. 6(b) shows the variation of C_{mag}/T with temperature. The C_{mag}/T decreases with decreasing temperature, but a broad peak is found at 12 K, at which the beginning of the divergence

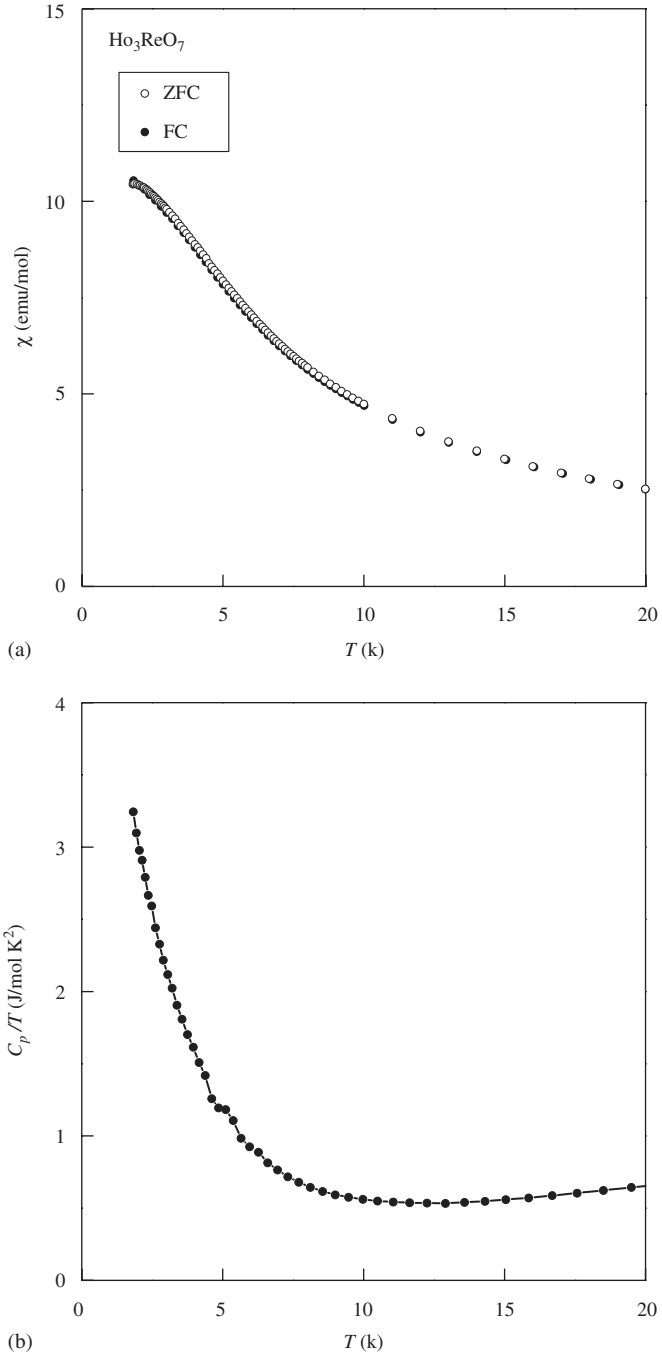

Fig. 7. (a) Temperature dependence of magnetic susceptibility for Ho_3ReO_7 below 20 K. (b) Temperature dependence of specific heat divided by temperature (C_p/T) for Ho_3ReO_7 below 20 K.

between the ZFC and FC susceptibilities against temperature was observed. Therefore, this behavior should be due to the magnetic properties of Re^{5+} ions in this compound.

3.2.3. Ho_3ReO_7

Figs. 7(a) and (b) show the low-temperature dependences of the magnetic susceptibility and the specific heat divided by temperature for Ho_3ReO_7, respectively. No magnetic anomaly is observed down to 1.8 K in the susceptibility vs. temperature curve, and no divergence between the ZFC and FC susceptibilities is found. On the other hand, the C_p/T increases with decreasing temperature down to 1.8 K below 10 K. This result may indicate the existence of magnetic ordering of Ho^{3+} below 1.8 K. For Ho_3TaO_7, its magnetic susceptibility and specific heat show the existence of a long-range magnetic transition at 2.6 K due to the magnetic interaction between Ho^{3+} ions [24].

4. Summary

Ln_3ReO_7 crystallized in an orthorhombic superstructure of cubic fluorite (space group *Cmcm* for $Ln = Sm$, Eu; $C222_1$ for $Ln = Ho$). The Sm_3ReO_7 shows an antiferromagnetic transition at 1.9 K. The Eu_3ReO_7 indicates a magnetic anomaly at 12 K. Both Sm_3ReO_7 and Eu_3ReO_7 undergo a structure transition at 270 and 350 K, respectively.

Acknowledgments

This work was supported by Grant-in-aid for Scientific Research of Priority Areas "Panoscopic Assembling and High Ordered Functions for Rare Earth Materials" no. 17042003 from the Ministry of Education, Science, Sports and Culture of Japan. This work was also partially supported by Grant-in-aid for Scientific Research, no. 18550049 from the Ministry of Education, Science, Sports and Culture of Japan.

References

[1] H.J. Rossell, J. Solid State Chem. 27 (1979) 115.
[2] F.P.F. van Berkel, D.J.W. IJdo, Mater. Res. Bull. 21 (1986) 1103.
[3] W.A. Groen, F.P.F. van Berkel, D.J.W. IJdo, Acta Crystallogr. C 43 (1986) 2262.
[4] P. Khalifah, R.W. Erwin, J.W. Lynn, Q. Huang, B. Batlogg, R.J. Cava, Phys. Rev. B 60 (1999) 9573.
[5] P. Khalifah, Q. Huang, J.W. Lynn, R.W. Erwin, R.J. Cava, Mater. Res. Bull. 35 (2000) 1.
[6] F. Wiss, N.P. Raju, A.S. Wills, J.E. Greedan, Int. J. Inorg. Mater. 2 (2000) 53.
[7] B.P. Bontchev, A.J. Jacobson, M.M. Gospodinov, V. Skumryev, V.N. Popov, B. Lorenz, R.L. Meng, A.P. Litvinchuk, M.N. Iliev, Phys. Rev. B. 62 (2000) 12235.
[8] D. Harada, Y. Hinatsu, J. Solid State Chem. 158 (2001) 245.
[9] D. Harada, Y. Hinatsu, Y. Ishii, J. Phys.: Condens. Matter 13 (2001) 10825.
[10] D. Harada, Y. Hinatsu, J. Solid State Chem. 164 (2002) 163.
[11] H. Nishimine, M. Wakeshima, Y. Hinatsu, J. Solid State Chem. 177 (2004) 739.
[12] W.R. Gemmill, M.D. Smith, H.-C. zur Loye, Inorg. Chem. 43 (2004) 4254.
[13] W.R. Gemmill, M.D. Smith, Y.A. Mozharivsky, G.J. Miller, H.-C. zur Loye, Inorg. Chem. 44 (2005) 7047.
[14] G. Wltschek, H. Paulus, I. Svoboda, H. Ehrenberg, H. Fuess, J. Solid State Chem. 125 (1996) 1.
[15] R. Lam, T. Langet, J.E. Greedan, J. Solid State Chem. 171 (2002) 317.
[16] Y. Hinatsu, M. Wakeshima, N. Kawabuchi, N. Taira, J. Alloys Compounds 374 (2004) 79.
[17] R.D. Shannon, Acta Crystallogr. A 32 (1976) 751.
[18] F. Izumi, T. Ikeda, Mater. Sci. Forum 198 (2000) 321.
[19] A. Kahn-Harari, L. Mazerrolles, D. Michel, F. Robert, J. Solid State Chem. 116 (1995) 103.
[20] J.E. Greedan, N.P. Raju, A. Wegner, P. Gougeon, J. Padiou, J. Solid State Chem. 129 (1997) 320.
[21] J.G. Allpress, H.J. Rossell, J. Solid State Chem. 27 (1979) 105.
[22] H. Nishimine, M. Wakeshima, Y. Hinatsu, J. Solid State Chem. 178 (2005) 1221.
[23] A. Abragam, B. Bleaney, Electron Paramagnetic Resonance of Transition Ions, Clarendon Press, Oxford, 1970.
[24] M. Wakeshima, Y. Hinatsu, J. Phys.: Condens. Matter 16 (2004) 4103.
[25] J.H. van Vleck, Theory of Electric and Magnetic Susceptibilities, Clarendon Press, Oxford, 1932.